Visibility Restoration in Infra-Red Images

Olivier Fourt and Jean-Philippe Tarel
COSYS-PICS-L
Univ. Gustave Eiffel, IFSTTAR
F-77454 Marne-la-Vallée, France
Email: jean-philippe.tarel@univ-eiffel.fr

***Abstract*—For the last decade, single image defogging has been a subject of interest in image processing. In the visible spectrum, fog and haze decrease the visibility of distant objects. Thus, the objective of the visibility restoration is to remove as much as possible the effect of the fog within the image. Infrared sensors are more and more used in automotive and aviation industries but the effect of fog and haze is not restricted to the visible spectrum and also applies in the infrared band. After recalling the effects of fog in the common sub-bands of the infrared spectrum, we tested if the approach used for single image defogging in the visible spectrum might also work for infrared. This led us to propose a new approach of single image defogging for Long-Wavelength Infra-Red (LWIR) or Thermal Infra-Red. Several experiments are presented showing that the proposed algorithm offers interesting results not only for fog and haze but for bad weather conditions in general, during day and night.**

I. Introduction

Driving a vehicle safely requires a quick and clear understanding of the surrounding environment, which is built from driver's perception. The driver can be also helped by vehicle sensors. Bad weather conditions may reduce the visual range and thus the distance at which a scene object can be detected and identified, in the visible spectrum. One decade ago, the question of how to process an image to remove the effects of fog and thus to enhance the visibility to distant objects became of interest. When processing only a single image, for instance from a moving camera, this problem is ill-posed and thus priors have to be introduced. This leads to heuristic approaches. The first two proposed approaches were [1], [2], quickly followed by [3], [4], [5] and other improvements or variants. Many of these approaches use a physically based model of the effect of daylight fog in an image, and thus can be considered as visibility restoration methods. This model is named Koschmieder's law [6]:

$$I(x) = I_0(x)t(x) + I_s(1 - t(x)) \tag{1}$$

where $I(x)$ is the observed intensity at pixel x, $I_0(x)$ is the intensity at close range, I_s is the intensity in the sky, t is the transmittance. The transmittance is $t(x) = e^{-k_d d(x)}$ where $d(x)$ is the distance to the camera and k_d is the scattering component of the extinction coefficient which characterizes daylight fog. This model is valid only when the fog is assumed uniform on the ray going through x, and when the lightening is also uniform along this ray. The k_d parameter is usually considered constant in the visible spectrum. Notice, that there is no fog when $k_d = 0$. If fog must be assumed constant on every pixel ray, k_d may vary from one pixel to another. The fog uniformity assumption is thus not necessarily required in the whole 3D scene to apply visibility restoration algorithms based on (1), see [7]. The last term in (1) is also know as the atmospheric veil.

In the AWARE (All Weather All Roads Enhanced vision) project, which focused on the design of a sensor enabling vision in all poor visibility conditions, such as night, fog, rain and snow, the benefit of using infrared sensors was demonstrated, see [8], [9]. In particular, it was observed inside the CEREMA's Fog chamber [10] that, for the same fog, the visibility distance increases from Visible spectrum to Near Infra-Red (NIR), from NIR to Short-Wavelength Infra-Red (SWIR) and from SWIR to Long-Wavelength Infra-Red (LWIR). This is due to the fact that if (1) still applies in several infrared sub-bands, the extinction coefficient must be considered as a function of the wavelength and this function is mainly decreasing [11].

In visibility restoration methods, an heuristic is usually proposed to guess the amount of white at each pixel and a percentage of this amount is used as an inference of the atmospheric veil. Then, (1) is used to obtain the formal link between atmospheric veil and transmittance, and thus to derive the restored image I_0 form the foggy image I. Such an approach is based on the fact that the atmospheric veil can be seen in the image, and only daylight foggy images can be processed correctly. When k_d is zero, as for LWIR, or close to zero as for Medium-Wavelength Infra-Red (MWIR), the atmospheric veil can not be observed. This implies that visibility restoration algorithms proposed for the visible spectrum, able to work on a gray level image, can be also applied with success to images from NIR and SWIR sensors, but not to images from MWIR and LWIR sensors. However, the LWIR band, also known as thermal band, is one of the most used infrared band, because of several available not too expensive uncooled LWIR sensors.

As a consequence, visibility restoration from a single LWIR image requires a dedicated approach. Well-known contrast enhancement algorithms can be used but are not dedicated to this specific task. For instance, algorithms have been proposed such as [12], [13], [14] based on standard enhancement algorithms [15]. The use of uncooled cameras makes images really noisy and it is not considered that the noise is emphasized during processing. Moreover, these previous algorithms are not based on a physical model of the fog effect and thus are not restoration methods.

A learning approach could have been considered but faces two major difficulties. First, there is a lack of image databases made of pairs of LWIR images with and without bad weather conditions of the same scene. Building small databases of this kind for evaluation is particularly complicated, as described in the experiments section. Second, the visibility restauration is a pre-processing step in the image processing pipeline that should be fast enought and inexpensive in calculations.

We thus propose an original approach of visibility restoration from a single LWIR image able to cope with the noise of uncooled LWIR cameras. Our method can restore contrast during day and night, and is based on a physical model of the fog effect, assuming a scene approximately planar, such as scenes observed from a ground vehicle. The proposed algorithm is very fast and inexpensive in term of calculation.

The paper is organized as follows: Sec. II addresses denoising, Sec. III describes the visibility restoration algorithm, and Sec. IV presents the experiments and comparison with several kinds of datasets. Even if the proposed algorithm is not particularly complicated, it performs well in almost any weather conditions.

II. Noise removal in LWIR

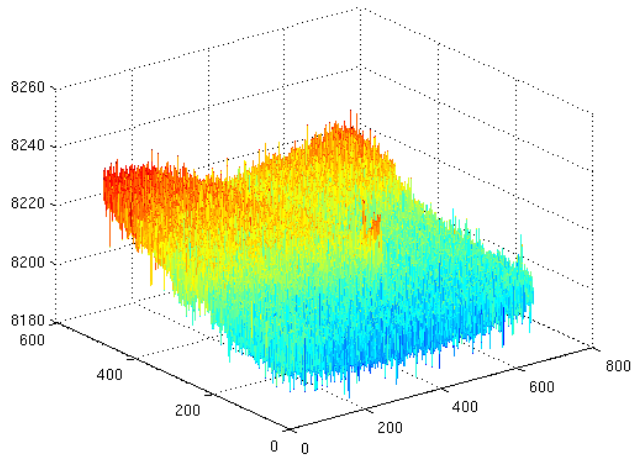

Fig. 1. LWIR image during bad weather in La Fageole pass, France, with a car centered in $(200, 400)$ pixel coordinates. The image in gray level is shown in Fig. 3.

Uncooled LWIR sensors are affected by a strong additive noise. This noise is not too visible in clear daylight scenes, but it can have the same magnitude as the signal in bad weather conditions, as shown in Fig. 1 and Fig. 3. Due to imperfect calibration of the sensor array, there is also a "raster effect", mainly on rows but also on columns, as visible in Fig. 3.

The probability distribution function (pdf) of the noise was obtained on image areas with constant signal, such as clear sky at night. As shown in Fig. 2, the noise pdf is close to a Gaussian pdf, centered, symmetric (skewness is in the range of 10^{-2}), with a standard deviation of 3, and a kurtosis close to 3.3. For noise removal, an edge-preserving local filter

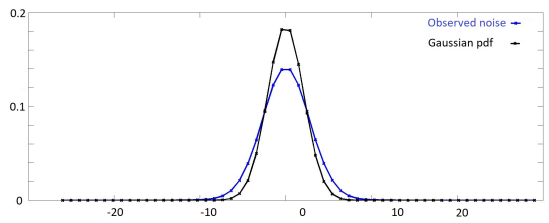

Fig. 2. Observed pdf of the noise in blue and Gaussian distribution with the same mean and standard deviation in black.

is required. We have implemented the bilateral filter with a constant weight in space and in intensity for 12-bit images. It is thus dedicated to the observed Gaussian noise [16]. We used a window size between 3 to 5 pixels, and an intensity threshold of 10. These values were selected experimentally. Fig. 3 shows the resulting denoising. On the left is the original noisy image during bad weather conditions, in La Fageole pass. On the right is the image after filtering. The filtered image is cleaner and some road signs are now more visible. Nevertheless all noise is not removed, not to remove image details.

Fig. 3. On the left is an original LWIR image in bad weather and on the right the denoised image after bilateral filtering.

Whatever the filter, we found that it is better to perform denoising before visibility restoration, otherwise the noise is amplified and its pdf is non-uniformly modified as a function of the pixel position in the image, making it more difficult to remove.

III. Visibility Restoration in LWIR

In LWIR, there is no atmospheric scattering. Therefore, $k_d = 0$ and thus Koschmieder's law (1) is useless. The effect of fog is mainly absorption in LWIR. The model of the effect of fog in LWIR band is therefore reduced to the Beer-Lambert's law [11]:

$$I(x) = I_0(x)e^{-k_a d(x)} \tag{2}$$

with the same notations as in (1), assuming a uniform fog of absorption coefficient k_a. From this model, one may think that a foggy LWIR image is similar to a night foggy image in the visible spectrum, without scattering and thus without halos. An extra term $I_a(T)(1 - e^{-k_a d(x)})$ should be added to the previous equation when the air is warm enough to produce a thermal veil. In such a case, its intensity I_a is related to the

Fig. 4. LWIR images in bright day (top) and in bad weather (bottom), La Fageole pass, France. From left to right, the original image, the image restored with the proposed algorithm and the image enhanced with CLAHE.

air temperature T. This extra term is negligible for outdoor scenes in temperate countries.

From (2), the effect of fog in LWIR is a multiplicative factor on the intensity which is related to the distance between the seen object and the camera, which is usually unknown and different from one pixel to another. The problem is thus ill-posed. Inspired by [2], we also assume that the scene is approximately and mainly horizontally planar. This assumption is most of the time verified for a camera in a vehicle looking at the road. The distance between the camera and the scene is thus constant along horizontal rows and the transmittance $t = e^{-k_a d(x)}$ is the same for all pixels along a row. Moreover, except at a few really hot objects such as vehicles, the intensity of a road scene is relatively locally smooth.

With these assumptions, a simple idea to restore the contrast in a foggy image is thus to apply a multiplicative corrective factor on every row, such that all rows get the same mean intensity (set for instance to the image mean). This algorithm was tested. It is very fast on standard pc without GPU and relatively efficient on bad weather images. Its complexity is linear in the number of image pixels. However, it produces artifacts (bright lines) when a hot and large object is in the scene. For the same reason, results obtained during clear daylight are also not always satisfying. The key problem with this algorithm is that the assumption of constant mean intensity along rows is not always true in LWIR images.

Our idea is thus to compute the corrective factor by assuming that intensity differences between two successive rows are small. This leads to an iterative process on rows, starting either from the top or the bottom of the image:

- Let $I(i,j)$ be the input image where (i,j) are a pixel coordinates.
- Let $R(i,j)$ be the restored image to be built.
- $R(1,\dots) = I(1,\dots)$ i.e the first row is not modified.
- For each row i from 2 to the last one, $R(i,\dots) = f_i I(i,\dots)$ with f_i the factor which minimizes the quadratic error between vectors $f_i I(i,\dots)$ and $R(i-1,\dots)$, i.e:

$$\arg\min_{f_i} \sum_j (f_i I(i,j) - R(i-1,j))^2 \tag{3}$$

which can be solved, by derivation, as:

$$f_i = \frac{\sum_j I(i,j) R(i-1,j)}{\sum_j I(i,j) I(i,j)} \tag{4}$$

This algorithm is applied twice on the same image, first from top to bottom and then from bottom to top. Then the final result is obtained as the mean of the top down and bottom up image results.

Minimizing the quadratic error between successive rows is valid when the same objects are seen in the two rows. If it is not the case, for instance because of a vertical contrast due to a new object in the second row, the estimated factor will be biased. To handle this difficulty, pixels with intensities that are too different from one row to another are discarded in the quadratic error. The threshold is computed from the image statistics or fixed.

Another difficulty lies in the remaining noise which induces small irregular variations of the factor from one row to another. To handle this, a smooth factor is obtained by a Gaussian

Fig. 5. LWIR image in CEREMA's Fog chamber [10]. On the left is the original image and on the right the restored image.

Fig. 6. Simulated LWIR images in dense fog with a visibility range of $30m$, by the company OKTAL SE. From left to right: image in visible band, original LWIR image, restored LWIR image.

smoothing with a spatial scale set experimentally to the value 18. A bounding is performed on factors with a difference too large with respect to the smooth factor. This leads to a trade-off between a good restoration and the amplification of the remaining noise.

IV. Experiments

Tests were performed on four kinds of image datasets from different uncooled LWIR cameras. Each dataset is made of several sequences of 12-bit images. These sequences are processed image per image and results are encoded in 16-bit images and 8-bit videos.

- The first dataset is made of videos recorded at the Col de La Fageole in France, for different kinds of weather (fog, rain, snow, clear sky…) with a VGA camera. The sequences were restored with the proposed algorithm. For comparisons, a selection of images were restored using other algorithms such as the Contrast Limited Adaptive Histogram Equalization algorithm (CLAHE [15]) and Multiscale Retinex algorithm [17].
- The second dataset is made of sequences recorded inside the CEREMA's Fog chamber [10], Clermont-Ferrand, with fog and rain using the same VGA camera and for a small half of the sequences, a $1/4$-VGA camera.
- The third dataset is made of simulated sequences built by the company OKTAL SE. These images are from a $1/4$-VGA camera. Several weather conditions are simulated: day and night, clear sky, cloud and fog. Being simulated, it is the only dataset were pairs of images with and without bad weather are available.
- The fourth dataset is made of sequences recorded outdoors in both urban and countryside environment, for several weather conditions (rain and night), with a $1/4$-VGA camera aboard of a vehicle.

Fig. 7. LWIR image with rain. From left to right, the original image, the image restored with the proposed algorithm and the image enhanced with CLAHE.

Tests on the first dataset have shown that, in bad weather conditions, the noise is high with respect to the signal. The evaluation and comparisons were qualitative since no reference is available. As illustrated in Fig. 4, the proposed algorithm brought better results compared with image enhancement using the Contrast Limited Adaptive Histogram Equalization algorithm (CLAHE [15]): images are less noisy, areas belonging to the same object are more homogeneous, less overcontrasts, background and sky remain separated. This is valid for daylight and night images. We also found that vehicles with high contrast passing through the scene do not affect the global image intensity along the video with the proposed algorithm. This is not the case with CLAHE. Besides, CLAHE is three time slower on average. We also tested the Multiscale Retinex algorithm [17] and observed that it strogly failed to cope with moving vehicles in videos.

Tests inside the fog chamber, see Fig. 5, and with the synthetic images, see Fig. 6, have shown a good robustness of the proposed algorithm despite that the planar world assumption is not verified due to buildings or people. Artifacts only appear at close range, under one meter. Results suggest to set a global max value to the factor f_i for rows higher than the line of horizon. Even with a really dense fog and a visibility distance of $30\ m$ in the visible spectrum, the visibility distance with the LWIR camera is higher than $100\ m$. This explains why fog is difficult to see in LWIR images in Fig. 5 and Fig. 6. Therfore, the comparison of the restauration with the LWIR reference image without fog is not very informative.

As shown in Fig. 7 and in Fig. 8, tests with the camera aboard the vehicle confirm the efficiency of the proposed algorithm despite camera motion. For instance in Fig. 7, people are easier to detect in the restored image with the proposed image compared to the original image and to the CLAHE enhanced image. In Fig. 8, cars and other scene objects are easier to detect in the restored image compared to the original image.

From the different databases, we obtained that the proposed restoration algorithm of LWIR images applies equally well to all kinds of bad weather conditions, such as fog, haze, rain and snow.

V. Conclusion

We showed that it is possible to directly apply single image defogging algorithms, designed in the visible spectrum, to infrared images in the NIR and SWIR bands, but not in the MWIR and LWIR bands. We thus propose the first visibility restoration algorithm dedicated to LWIR images in the context of driving scenes. The proposed algorithm is fast enought, inexpensive in term of calculation and thus adequate to be embeded within vehicles. It takes into account that LWIR camera can be uncooled and thus with a low signal to noise ratio in bad weather conditions. Contrary to single image defogging in the visible spectrum, the proposed algorithm is able to cope with daytime as well as nighttime scenes. The proposed restoration algorithm applies to images with fog, haze, and all kinds of bad weather conditions such as rain and snow. During our tests, the proposed algorithm achieved good performance for driver visualization, in several good or bad weather conditions. This process is under patent application [18].

Possible improvements include: better denoising using a better model of the artifacts caused by micro-bolometer calibration, and optimization of the denoising and restoration algorithms. We think that visibility restoration algorithms for LWIR cameras should improve the efficiency of several Advanced Driver-Assistance Systems. The visibility restoration in the MWIR band, as well as in LWIR in presence of a thermal veil, which are two problems where scattering and absorption are combined, is an open subject of interest.

Acknowledgment

The authors would like to thank FUI project AWARE (All Weather All Roads Enhanced vision) for funding.

References

[1] R. Tan, N. Pettersson, and L. Petersson, "Visibility enhancement for roads with foggy or hazy scenes," in *Proceedings of the IEEE Intelligent Vehicles Symposium (IV'07)*, Istanbul, Turkey, 2007, pp. 19–24.

[2] N. Hautière, J.-P. Tarel, and D. Aubert, "Towards fog-free in-vehicle vision systems through contrast restoration," in *IEEE International Conference on Computer Vision and Pattern Recognition (CVPR'07)*, Minneapolis, Minnesota, USA, Jun. 2007, pp. 1–8. [Online]. Available: http://perso.lcpc.fr/tarel.jean-philippe/publis/cvpr07.html

[3] R. Fattal, "Single image dehazing," in *ACM SIGGRAPH'08*. New York, NY, USA: ACM, 2008, pp. 1–9.

Fig. 8. Examples of LWIR image in bad weather from a camera embedded in a car: original image (left) and restored image (right).

[4] K. He, J. Sun, and X. Tang, "Single image haze removal using dark channel prior," in *IEEE Conference on Computer Vision and Pattern Recognition (CVPR'09)*, Miami Beach, Florida, USA, 2009, pp. 1956–1963.

[5] J.-P. Tarel and N. Hautière, "Fast visibility restoration from a single color or gray level image," in *IEEE International Conference on Computer Vision (ICCV'09)*, Kyoto, Japan, Sep. 2009, pp. 2201–2208. [Online]. Available: http://perso.lcpc.fr/tarel.jean-philippe/publis/iccv09.html

[6] W. E. K. Middleton, *Vision Through the Atmosphere*. University of Toronto Press, 1952.

[7] J.-P. Tarel, N. Hautière, L. Caraffa, A. Cord, H. Halmaoui, and D. Gruyer, "Vision enhancement in homogeneous and heterogeneous fog," *IEEE Intelligent Transportation Systems Magazine*, vol. 4, no. 2, pp. 6–20, Jun. 2012. [Online]. Available: http://perso.lcpc.fr/tarel.jean-philippe/publis/itsm12.html

[8] N. Pinchon, M. Ibn-Khedher, O. Cassignol, A. Nicolas, F. Bernardin, P. Leduc, J.-P. Tarel, R. Brémond, E. Bercier, and Julien, "All-weather vision for automotive safety: which spectral band?" in *Proceedings of SIA Vision (VISION'16)*, Paris, France, Oct. 2016. [Online]. Available: http://perso.lcpc.fr/tarel.jean-philippe/publis/vision16.html

[9] N. Pinchon, , O. Cassignol, A. Nicolas, F. Bernardin, P. Leduc, J.-P. Tarel, R. Brémond, E. Bercier, and J. Brunet, "All-weather vision for automotive safety: which spectral band?" in *Proceedings of 22nd International Forum on Advanced Microsystems for Automotive Applications (AMAA'18)*, Berlin, Germany, 2018, pp. 3–15. [Online]. Available: http://perso.lcpc.fr/tarel.jean-philippe/publis/amaa18.html

[10] M. Colomb, K. Hirech, P. André, J. Boreux, P. Lacote, and J. Dufour, "An innovative artificial fog production device improved in the european project FOG," *Atmospheric Research*, vol. 87, no. 3-4, pp. 242–251, 2008.

[11] E. Bernard, "Comparaison théorique et expérimentale des performances après traitement de l'imagerie active et de l'IR2 en conditions dégradées," Ph.D. dissertation, Université de Toulouse III-Paul Sabatier, 2015.

[12] K.-H. Kim, S.-W. Lee, C.-G. Noh, Y.-J. Kim, and B. Lee, "Driver's thermal vision enhancement using concentration region on the vehicles," in *Sensors, 2006. 5th IEEE Conference on*. IEEE, 2006, pp. 1167–1170.

[13] G.-H. Park and J.-S. Youn, "A fast contrast enhancement method for forward looking infrared imaging system," in *Infrared, Millimeter, and Terahertz Waves, 2009. IRMMW-THz 2009. 34th International Conference on*. IEEE, 2009, pp. 1–2.

[14] L. Shanshan, W. Jintao, and S. Liming, "A new infrared image enhancement algorithm," in *Control and Decision Conference (CCDC), 2016 Chinese*. IEEE, 2016, pp. 5111–5114.

[15] S. M. Pizer, E. P. Amburn, J. D. Austin, R. Cromartie, A. Geselowitz, T. Greer, B. ter Haar Romeny, J. B. Zimmerman, and K. Zuiderveld, "Adaptive histogram equalization and its variations," *Computer vision, graphics, and image processing*, vol. 39, no. 3, pp. 355–368, 1987.

[16] L. Caraffa, J.-P. Tarel, and P. Charbonnier, "The guided bilateral filter: When the joint/cross bilateral filter becomes robust," *IEEE Transactions on Image Processing*, vol. 24, no. 4, pp. 1199–1208, 2015.

[17] D. J. Jobson, Z.-u. Rahman, and G. A. Woodell, "A multiscale retinex for bridging the gap between color images and the human observation of scenes," *IEEE Transactions on Image processing*, vol. 6, no. 7, pp. 965–976, 1997.

[18] O. Fourt and J.-P. Tarel, "Procédé et dispositif de traitement d'images," French patent registration number FR1913539, IFSTTAR, Nov. 2019.